A Faceted Prior for Scalable Wideband Computational Imaging

Pierre-Antoine Thouvenin*, Abdullah Abdulaziz*, Ming Jiang†, Audrey Repetti‡*, and Yves Wiaux*

*Institute of Sensors, Signals and Systems, Heriot-Watt University, Edinburgh EH14 4AS, United Kingdom.
†Signal Processing Laboratory 5 (LTS5), École Polytechnique Fédérale de Lausanne, CH-1015, Lausanne, Switzerland.
‡Department of Actuarial Mathematics & Statistics, Heriot-Watt University, Edinburgh EH14 4AS, United Kingdom.

Abstract—**Hyperspectral images exhibit strong spectral correlations, which can be exploited *via* a low-rankness and joint-sparsity prior when reconstructed from incomplete and noisy measurements. A state-of-the-art solution consists in using a regularization term based on both the $\ell_{2,1}$ and the nuclear norms, which however does not scale well with large numbers of spectral channels and huge image sizes. To alleviate this issue, we propose a parallelizable faceted low-rankness and joint-sparsity prior to improve the scalability of the associated imaging algorithm while preserving its reconstruction performance and better promoting local spectral correlations. We illustrate our approach on synthetic data in the context of radio-astronomy.**

I. A SCALABLE LOW-RANKNESS AND JOINT-SPARSITY PRIOR

Context and motivations. Hyperspectral (HS) imaging consists in recovering an image in several contiguous spectral channels from a set of noisy, possibly incomplete measurements. The problem can be cast as the following generic optimization task

$$\underset{\boldsymbol{X}\in\mathbb{R}_+^{N\times L}}{\text{minimize}}\ f(\mathbf{Y},\boldsymbol{\Phi X}) + r(\boldsymbol{X}) \qquad (1)$$

where N is the image size, L is the number of spectral channels, $\boldsymbol{X}$ is the unknown HS image, $\boldsymbol{\Phi}\in\mathbb{C}^{M\times N}$ represents a linear measurement operator and $\mathbf{Y}\in\mathbb{C}^{M\times L}$ are the measurements. The functions f and r are respectively the data fitting and the regularization terms, encoding additional prior on the structure of $\boldsymbol{X}$. In many applications, $\boldsymbol{X}$ exhibits significant spectral correlations, which can be exploited in the estimation process [1]–[4]. An efficient approach consists in resorting to low-rank and joint-sparse regularizations based on both the nuclear and $\ell_{2,1}$ norms [5]: $r(\boldsymbol{X})=\lambda\|\boldsymbol{X}\|_* +\mu\|\boldsymbol{\Psi}^\dagger\boldsymbol{X}\|_{2,1}$, where $\boldsymbol{\Psi}^\dagger\in\mathbb{R}^{P\times N}$ represents a sparsifying dictionary. To solve the resulting problem, [6] proposed an iterative primal-dual (PD) algorithm, which can handle all the functions in parallel without needing sub-iterations or to invert the linear operators involved [7]. Nevertheless, handling r may be computationally demanding in practice, and consequently not suitable in a very high dimensional setting. Radio-astronomy is an extreme example: new generation of radio telescopes are expected to provide surveys with sub-arcsec resolution over thousands of frequency channels, producing widefield images composed of 10^{14} pixels for the Square Kilometer Array (SKA) [8]. To overcome this issue, scalable alternatives to the nuclear norm have been proposed in the literature. In [9], the nuclear norm is formulated as a solution to a scalable non-convex problem. However, due to the non-convexity, methods such as the primal-dual algorithm cannot be used. Alternatively, in [10] a scalable low-rank framework based on graph signal processing is introduced when the measurements are in the image domain, which is not the case for applications such as radio-astronomy (where observations are acquired in the Fourier domain).

Proposed approach. We propose a simple facet-based version of the $\ell_{2,1}$ and nuclear norm regularization expressed as

$$r(\boldsymbol{X}) = \sum_{i=1}^{I} \lambda_i\|\mathbf{W}_i\tilde{\mathbf{S}}_i\boldsymbol{X}\|_* + \mu_i\|\boldsymbol{\Psi}_i^\dagger\mathbf{S}_i\boldsymbol{X}\|_{2,1} \qquad (2)$$

where the masking operators $\{\tilde{\mathbf{S}}_i,\mathbf{S}_i\}_{i=1}^I$ produce spatially overlapping groups of pixels (i.e., rows of $\boldsymbol{X}$) referred to as facets, whose definition is application-dependent. The diagonal weighting matrices $\{\mathbf{W}_i\}_{i=1}^I$ are aimed at ensuring a smooth transition between facets to reduce potential tessellation artifacts. Different decomposition strategies can be adopted, e.g., tailored for the structure of the initial dictionary $\boldsymbol{\Psi}^\dagger$ (when $\boldsymbol{\Psi}^\dagger$ is a wavelet transform, it can be exactly decomposed in terms of facet-based wavelet transforms $\boldsymbol{\Psi}_i^\dagger$ [11]). This prior offers additional degrees of parallelism to algorithms based on variable splitting [12], in particular for the PD algorithm [13].

Indeed, leveraging advanced PD functionalities, at each iteration, each term of the objective function (i.e. each facet) can be handled independently in parallel before being aggregated to ensure convergence to a solution to the global problem (1). Thus, combining the proposed faceting prior to the PD algorithm reduces both the memory requirement for the estimated HS image and the computational cost per iteration, leading to a new highly scalable method for HS imaging.

II. APPLICATION TO WIDEBAND RADIO-ASTRONOMY

We leverage (2) to solve the wideband imaging problem (1) for radio-astronomy. The proposed approach can be seen as a scalable version of the PD algorithm HyperSARA [6] with a facet-based prior that better promotes local spectral correlation. In this context, f models an ℓ_2 constraint. The SARA prior [14] involved in HyperSARA, based on wavelet transforms, leads to define $\{\mathbf{S}_i\}_{i=1}^I$ as in [11] to ensure an exact decomposition of the $\ell_{2,1}$ term. The operators $\{\tilde{\mathbf{S}}_i\}_{i=1}^I$ are defined with a larger overlap to mitigate reconstruction artifacts resulting from the tessellation of the nuclear norm.

Simulation settings. Following [6], we simulate a wideband model image of the W28 supernova remnant composed of $N = 1024\times1024$ pixels and $L = 20$ spectral channels. The measurement operator corresponds to a realistic spatial Fourier sampling, where $M\approx0.5N$. The data are corrupted by an additive zero-mean white Gaussian noise, leading to a signal-to-noise ratio (SNR) of 60 dB. To evaluate the interest of (2), we compare the reconstruction performance of a primal-dual algorithm to solve (1) with: (i) $r(\boldsymbol{X}) = \mu\|\boldsymbol{\Psi}^\dagger\boldsymbol{X}\|_{1,1}$, $\mu = 10^{-3}$ (corresponding to SARA [14]) (ii) $r(\boldsymbol{X}) = \lambda\|\boldsymbol{X}\|_* + \mu\|\boldsymbol{\Psi}^\dagger\boldsymbol{X}\|_{2,1}$ (HyperSARA [6]), with $(\lambda,\mu) = (1,10^{-3})$; (iii) the proposed faceted prior defined in (2), with $I = 16$ facets (4 along each spatial dimension), and $(\lambda_i,\mu_i) = (1,10^{-5})$ for $i\in\{1,\ldots,I\}$.

Experimental results. The reconstructed images and error images obtained with the three methods in channels 1 and 20 are reported in Fig. 1, along with the reconstruction SNR and per-iteration reconstruction time. The proposed approach yields a reconstruction quality similar to HyperSARA (outperforming SARA), for a computing time closer to SARA, the fastest approach. The error images specifically highlight the efficiency of the proposed approach in reconstructing very low intensity emission, possibly in relation with a better handling of local spectral correlations.

Conclusion and perspectives. We have proposed a highly scalable HS imaging method, based on a faceting prior promoting both low-rankness and joint-sparsity of the HS image of interest. We have shown that the proposed approach improves scalability of the state-of-the-art HS method in radio-astronomical imaging, while preserving its reconstruction performance. Additional experiments will be conducted in future works to better appreciate the performance of the proposed faceting approach. In particular, randomization could be leveraged to control the number of facets handled at each iteration.
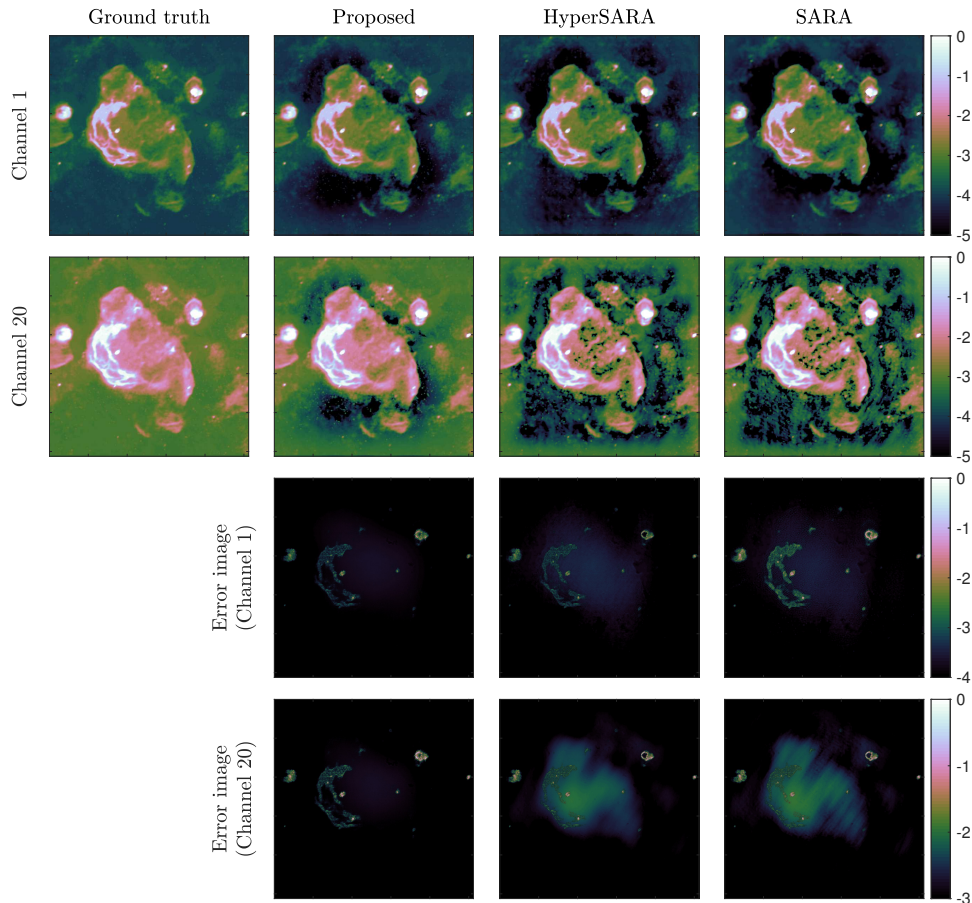
Fig. 1. Reconstructed (first two rows) and error images (last rows) displayed in log scale for the different approaches (in column: ground truth, proposed approach, HyperSARA and SARA). The reconstruction SNR for the displayed channels and per iteration computing time are: (proposed) [36.97/36.97 dB, 7.8 s], (HyperSARA) [SNR = 38.83/37.83 dB, 45 s], (SARA) [27.78/37.06 dB, 2.2 s]. Although the SNR reported for the proposed approach is smaller than the one of HyperSARA, the images obtained with the former approach show an overall improvement in the reconstruction quality of low intensity pixels for a much lower computing time than HyperSARA. The reconstruction performance of SARA is sub-optimal for wideband imaging since the correlation of the wideband data is not exploited, and given the nature of Fourier sampling in radio-astronomy where high Fourier modes are probed at higher frequency channels and low Fourier modes are probed at low frequency channels.

REFERENCES

[1] M. Golbabaee, S. Arberet, and P. Vandergheynst, "Compressive source separation: Theory and methods for hyperspectral imaging," *IEEE Trans. Image Process.*, vol. 22, no. 12, pp. 5096–5110, Dec. 2013.

[2] M. Kleinsteuber and H. Shen, "Blind source separation with compressively sensed linear mixtures," *IEEE Signal Process. Lett.*, vol. 19, no. 2, pp. 107–110, Feb. 2012.

[3] M. Jiang, J. Bobin, and J.-L. Starck, "Joint multichannel deconvolution and blind source separation," *SIAM J. Imaging Sci.*, vol. 10, no. 4, pp. 1997–2021, 2017.

[4] A. Abdulaziz, A. Dabbech, A. Onose, *et al.*, "A low-rank and joint-sparsity model for hyper-spectral radio-interferometric imaging," in *Proc. European Signal Process. Conf. (EUSIPCO)*, Budapest, Hungary, Aug. 2016, pp. 388–392.

[5] M. Golbabaee and P. Vandergheynst, "Hyperspectral image compressed sensing via low-rank and joint-sparse matrix recovery," in *Proc. IEEE Int. Conf. Acoust., Speech, and Signal Processing (ICASSP)*, Kyoto, Japan, Mar. 2012, pp. 2741–2744.

[6] A. Abdulaziz, A. Dabbech, and Y. Wiaux, "Wideband super-resolution imaging in radio interferometry via low rankness and joint average sparsity models (HyperSARA)," 2018, submitted. [Online]. Available: https://arxiv.org/abs/1806.04596.

[7] L. Condat, "A primal-dual splitting method for convex optimization involving Lipschitzian, proximable and linear composite terms," *J. Optim. Theory Appl.*, vol. 158, pp. 460–479, 2013.

[8] P. Dewdney, W. Turner, R. Millenaar, *et al.*, "SKA1 system baseline design," *Document number SKA-TEL-SKO-DD-001 Revision*, vol. 1, no. 1, 2013.

[9] F. Shang, Y. Liu, and J. Cheng, "Scalable algorithms for tractable Schatten quasi-norm minimization," in *Proceedings of the Thirtieth AAAI Conference on Artificial Intelligence*, 2016, pp. 2016–2022.

[10] N. Shahid, F. Grassi, and P. Vandergheynst, "Multilinear low-rank tensors on graphs & applications," *arXiv preprint*, 2016. [Online]. Available: https://arxiv.org/abs/1611.04835.

[11] Z. Pruša, "Segmentwise discrete wavelet transform," PhD thesis, Brno university of technology, 2012.

[12] P. L. Combettes and J.-C. Pesquet, "Proximal splitting methods in signal processing," *Fixed-Point Algorithms for Inverse Problems in Science and Engineering*, vol. 49, pp. 185–212, May 2011.

[13] J.-C. Pesquet and A. Repetti, "A class of randomized primal-dual algorithms for distributed optimization," *Journal of nonlinear and convex analysis*, vol. 16, no. 12, pp. 2453–2490, Nov. 2015.

[14] R. E. Carrillo, J. D. McEwen, and Y. Wiaux, "Sparsity Averaging Reweighted Analysis (SARA): A novel algorithm for radio-interferometric imaging," *Monthly Notices of the Royal Astronomical Society*, vol. 426, no. 2, pp. 1223–1234, 2012.